13th National Conference on
EARTHQUAKE ENGINEERING
PORTLAND, OREGON | JULY 13-17, 2026

Resilience Through Community Engagement and Technology

Directionality Characteristics of Near-Fault Simulated Ground Motions from Physics-Based Hayward Fault Rupture Simulations

M. Herrera[1] and M. Kenawy[2]

ABSTRACT

The spectral intensity of earthquake ground motions and corresponding seismic demands on structures can vary significantly with changes in the horizontal orientation, and this variation may exhibit sensitivity to the associated rupture distance and vibration period. We use a database of physics-based Hayward fault rupture simulations with broadband, spatially dense ground acceleration records to study the polarization characteristics of near-fault ground motions in strike-slip events, and their spatial and period-dependent variation. Preliminary results show strong polarization toward the strike-normal orientation in the near-fault region, and toward the transverse epicentral orientation across a longer distance range. The directionality characteristics of the spectral accelerations of simulated ground motions were found to be generally consistent with those of real ground motions observed in the near-fault region.

Introduction

The intensity of horizontal earthquake ground shaking and the imposed seismic demands on structures exhibit variation with changes in orientation within the horizontal plane. Quantifying this variation, conventionally known as ground motion directionality, is important for the seismic analysis and design of structures, especially those in regions of high seismic hazard [1]. The directionality of horizontal ground motion has traditionally been characterized by the direction of maximum spectral acceleration (SA) over all possible orientations [2], [3], [4], [5], [6], [7], [8]. Over the past two decades, studies of recorded ground motions have also documented the spatial variation of the direction of maximum SA across rupture distances. Early studies found that the maximum SAs at relatively short periods did not have a preferred orientation at distances longer than 5 km from the fault [3], [9]. At distances shorter than 5 km, the orientation of the maximum SA tended to be close to the strike-normal (SN) orientation [3], [9], [10], and the SN component intensity was frequently observed to be higher than the strike-parallel (SP) component intensity for strike-slip events. This polarization in near-fault ground motion was generally attributed to the seismic wave propagation patterns causing the well-known forward rupture directivity effects, which induce strong velocity pulses at near-fault locations [11], [12]. Although the polarization of horizontal ground motion was typically observed in the near-fault region, analysis of the 2010 Darfield earthquake [3] revealed that it persisted at rupture distances (R_{rup}) up to 30 km for SAs at periods longer than 1.0 second. More recent investigations [3], [5], [7], [16] found that the direction of

[1] Graduate Student Researcher, Dept. of Civil and Environmental Engineering, Oklahoma State University, Stillwater, OK 74078 (email: mherr18@okstate.edu)
[2] Assistant Professor, Dept. of Civil and Environmental Engineering, Oklahoma State University, Stillwater, OK 74078 (email: mkenawy@okstate.edu)

Herrera M, Kenawy M. Directionality Characteristics of Near-Fault Simulated Ground Motions from Physics-Based Hayward Fault Rupture Simulations. *Proceedings of the 13th National Conference in Earthquake Engineering*, Earthquake Engineering Research Institute, Portland, OR. 2026.

maximum SA in several densely recorded earthquakes at R_{rup} > 30 km occurred near the so-called transverse epicentral orientation, which is the distance perpendicular to a straight line drawn from the site to the epicenter.

Although the spatial variation of ground motion directionality has been studied in several earthquake events, recordings of near-fault ground motions are relatively sparse. In addition, the systematic effects of different rupture characteristics are difficult to isolate from individual event observations. Physics-based fault rupture simulations [13], [14], [15] offer new opportunities for studying the directionality features of ground motion intensity measures, especially at near-fault locations. These simulations offer spatially dense and site-specific recordings across large geographical regions, and can isolate systematic source, path, and site effects. In this study, we examine the directionality of near-fault ground motions in a database of physics-based fault-rupture simulations, which represent multiple realizations of a magnitude 7 (M7) Hayward fault rupture across the San Francisco Bay Area (SFBA) [16]. We use the database to analyze the spatial and period-dependent polarization of near-fault simulated ground motions, compare their directionality characteristics to those associated with real ground motion records, and discuss the implications of the observed trends.

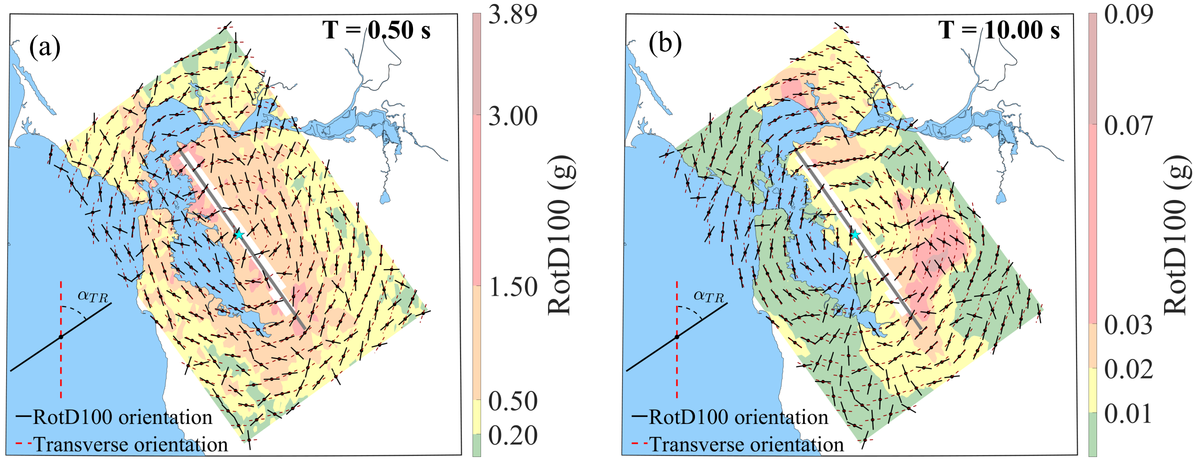

Figure 1. Amplitude and orientation of RotD100 across the SFBA at two vibration periods: (a) 0.5 seconds and (b) 10 seconds. The star indicates the epicenter location.

Physics-Based Fault Rupture Simulations

We obtained the fault rupture simulations from the Simulated Ground Motion Database managed by the Pacific Earthquake Engineering Research Center (PEER) and Lawrence Berkeley National Laboratory [16]. These simulations have undergone substantial validation efforts in recent years [16], [17], [18]. We use fifty rupture realizations which represent variations in the hypocenter location, slip distribution across the fault surface, and presence and size of slip asperities (patches). Each realization contains recordings at 2,270 stations spaced at 2 km over a 120-km by 80-km spatial domain. The simulations use the United States Geological Survey SFBA velocity model [19], and resolve frequencies up to 5 Hz with a minimum shear-wave velocity of 250 m/s.

Spatial and Period-Dependent Variability of Ground Motion Directionality

We describe the directionality of ground motion intensity by the direction of the orientation-independent maximum SA (RotD100) [1] for a 5%-damped oscillator with vibration periods between 0.2 and 10 seconds. The horizontal ground motion components were rotated through all possible angles between 0 and 180°, and the orientation and amplitude of RotD100 were recorded. We calculated the minimum angular difference between the RotD100 direction and two reference orientations: (1) the transverse epicentral orientation α_{TR}; and (2) the SN orientation α_{SN}. A representative example of the orientation of RotD100 is shown in Figure 1 for a single rupture realization and two vibration periods: 0.5 and 10 seconds. The transverse epicentral orientation is also shown for reference. Analysis of the RotD100 direction in all rupture realizations highlights its variation with the associated rupture distance. This observation is summarized in Figure 2, which displays the probability density of α_{TR} and α_{SN} for RotD100 at all vibration periods and two groups of R_{rup}. We observe that the direction of RotD100 tends to be close to the epicentral transverse direction, especially at near-fault locations (Figure 2a): the median α_{TR} is equal to 27 degrees for rupture distances shorter than 5 km, and 36 degrees for rupture distances longer than 5 km. In reference to the SN orientation (Figure 2b and 2d), the RotD100 direction of near-fault ground motions (R_{rup}< 5 km) also tends to be close to the SN direction (median α_{SN}= 28 degrees), which agrees with the observations of Bradley and Baker [2] and Watson-Lamprey and Boore [19] for real near-fault ground motions. However, at rupture distances longer than 5 km, the RotD100 direction is slightly closer to the SP direction (median α_{SN} = 52 degrees).

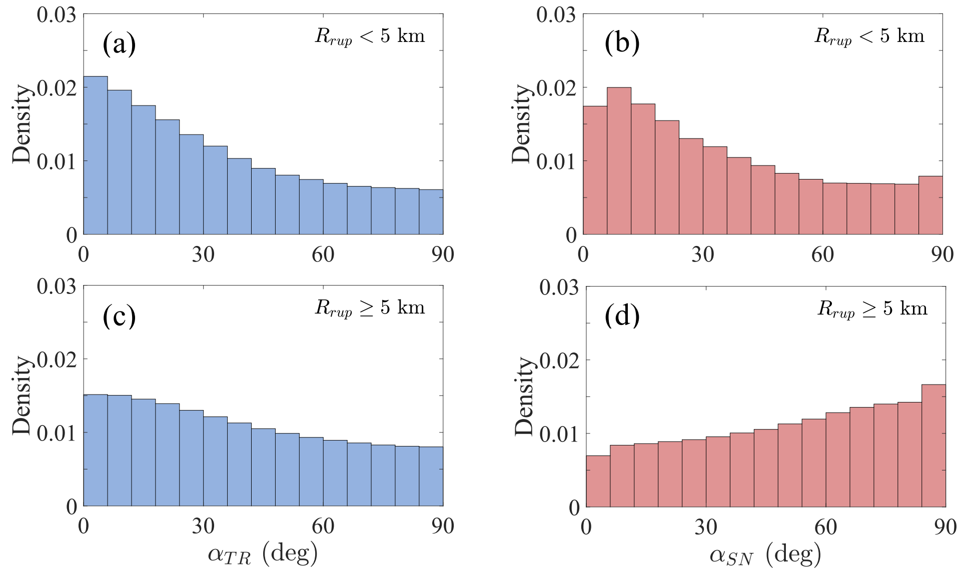

Figure 2. Probability density of the angle between RotD100 and the reference orientations: (a) α_{TR} at R_{rup} < 5 km; (b) α_{SN} at R_{rup} < 5 km; (c) α_{TR} at $R_{rup} \geq 5$ km; and (d) α_{SN} at $R_{rup} \geq 5$ km.

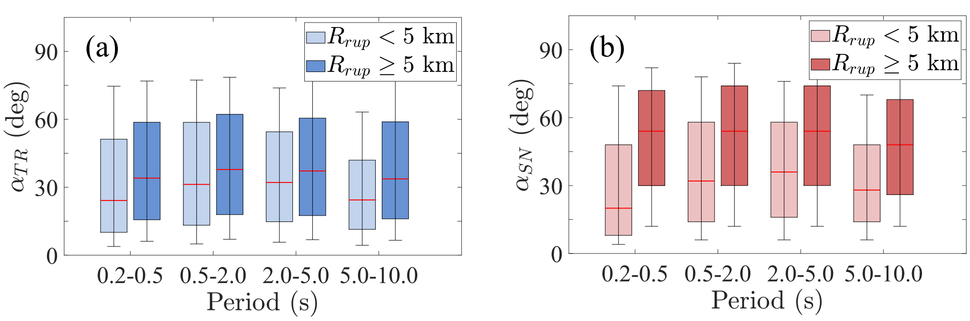

Figure 3. Angle between RotD100 and the reference orientations for multiple vibration periods and rupture distance bins: (a) α_{TR} (b) α_{SN}. Boxes mark the 25th, 50th, and 75th percentiles, and whiskers mark the 10th and 90th percentiles.

We also observe that the angular distance between the RotD100 direction and epicentral transverse orientation remains consistent across different vibration periods, with the median α_{TR} values ranging from 24 to 38 degrees. These trends are summarized in Figure 3a for multiple vibration period bins within the two rupture-distance groups. In contrast, the angular distance between the RotD100 direction and SN orientation exhibits a stronger sensitivity to both the rupture distance and vibration period range (Figure 3b). For R_{rup} < 5 km, the RotD100 direction tends to be close to the SN orientation, especially at periods shorter than or equal to

0.5 seconds (median α_{SN} = 18 degrees for $T \leq 0.5$ s). However, at rupture distances longer than 5 km, most α_{SN} values at all vibration periods do not exhibit a directional preference or are slightly closer to the SP orientation. Specifically, the median α_{SN} values for the four period bins in Figure 3b range between 48 and 54 degrees. These observations suggest that the epicentral transverse orientation may offer a more consistent metric for describing the spectral acceleration (SA) directionality across a wide range of distances and vibration periods, compared with the SN direction typically adopted for near-fault ground motions.

Comparison between Simulated and Recorded Ground Motions

The directionality characteristics of the simulated ground motions were also compared against a group of recorded ground motions from the PEER NGA-West2 database [20], which consists of 87 pairs of records with magnitudes between 6.2 and 7.7 (median magnitude of 6.9), R_{rup} between 0 and 30 km, and average shear-wave velocity in the top 30 meters (V_{s30}) between 250 and 1200 m/s. A subset of 1,500 pairs of simulated ground motions was randomly sampled to closely match the distribution of R_{rup} and V_{s30} of the PEER NGA-West2 records. Figure 4 summarizes the trends of the angular distance between the RotD100 and SN direction for both groups at multiple distance bins and periods of 0.5, 5.0, and 10.0 seconds. We observe that the differences between the directionality patterns associated with the simulated and recorded ground motions are sensitive to the associated rupture distance and vibration period. It is, however, noteworthy that the box plots for R_{rup}< 5 km contain only 12 real ground motions. Based on the Kolmogorov-Smirnov test at the 5% confidence level, we observe no statistically significant difference in the orientation of the RotD100 between the simulated and real ground motions for most periods between 0.2 and 10 seconds at rupture distances shorter than 15 km. On the other hand, for rupture distances longer than 15 km, a statistically significant difference is observed between the two groups at most periods. However, the size of the difference is considered small to medium, based on Cliff's Delta effect size measure d ($|d|$ < 0.35). These findings suggest that the directionality patterns of near-fault simulated ground motions are generally consistent with those of real ground motions.

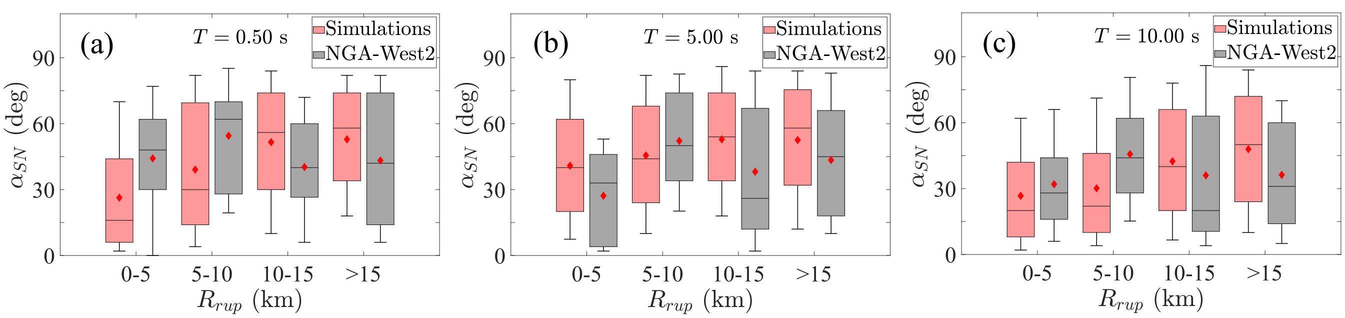

Figure 4. Angular distance between the RotD100 and SN orientations for simulated and real ground motions at the following vibration periods: (a) T = 0.5 s; (b) T = 5.0 s; and (c) T = 10.0 s. Boxes mark the 25th, 50th, and 75th percentiles, and the mean is indicated by the red dot.

Conclusions

Analysis of physics-based Hayward fault rupture simulations reveals that their ground motion directionality patterns are generally consistent with those of recorded ground motions, especially in the near-fault region. The RotD100 direction in the simulated ground motions exhibits substantial spatial variability and strong polarization toward the SN direction in the near-fault region, but this polarization diminishes at rupture distances longer than 5 km. Our analysis also suggests that the epicentral transverse direction may offer a more consistent reference orientation for characterizing the directionality of simulated ground motion intensity across a wide range of distances and vibration periods, compared with the SN orientation. Future work will examine the influence of rupture characteristics, such as the hypocenter location and spatial distribution of slip, on the polarization of the intensity measures of simulated ground motions.

References

[1] D. M. Boore, "Orientation-Independent Measures of Ground Motion," *Bull. Seismol. Soc. Am.*, vol. 96, no. 4A, pp. 1502–1511, Aug. 2006, doi: 10.1785/0120050209.

[2] Y.-N. Huang, A. S. Whittaker, and N. Luco, "Maximum Spectral Demands in the Near-Fault Region," *Earthq. Spectra*, vol. 24, no. 1, pp. 319–341, Feb. 2008, doi: 10.1193/1.2830435.

[3] B. A. Bradley and J. W. Baker, "Ground motion directionality in the 2010–2011 Canterbury earthquakes," *Earthq. Eng. Struct. Dyn.*, vol. 44, no. 3, pp. 371–384, Mar. 2015, doi: 10.1002/eqe.2474.

[4] N. Girmay, A. Poulos, and E. Miranda, "Directionality and polarization of response spectral ordinates in the 2023 Kahramanmaras, Türkiye earthquake doublet," *Earthq. Spectra*, vol. 40, no. 1, pp. 486–504, Feb. 2024, doi: 10.1177/87552930231203989.

[5] A. Poulos and E. Miranda, "Effect of Style of Faulting on the Orientation of Maximum Horizontal Earthquake Response Spectra," *Bull. Seismol. Soc. Am.*, vol. 113, no. 5, pp. 2092–2105, Oct. 2023, doi: 10.1785/0120230001.

[6] A. Poulos and E. Miranda, "Probabilistic characterization of the directionality of horizontal earthquake response spectra," *Earthq. Eng. Struct. Dyn.*, vol. 51, no. 9, pp. 2077–2090, Jul. 2022, doi: 10.1002/eqe.3654.

[7] A. Poulos, E. Miranda, and J. W. Baker, "Evaluation of Earthquake Response Spectra Directionality Using Stochastic Simulations," *Bull. Seismol. Soc. Am.*, vol. 112, no. 1, pp. 307–315, Feb. 2022, doi: 10.1785/0120210101.

[8] A. Poulos and E. Miranda, "Directionality characteristics of horizontal response spectra from the 2022 M_w 6.9 Chihshang, Taiwan earthquake," *Earthq. Spectra*, vol. 40, no. 3, pp. 1683–1696, Aug. 2024, doi: 10.1177/87552930241247478.

[9] S. K. Shahi and J. W. Baker, "NGA-West2 Models for Ground Motion Directionality," *Earthq. Spectra*, vol. 30, no. 3, pp. 1285–1300, Aug. 2014, doi: 10.1193/040913EQS097M.

[10] J. A. Watson-Lamprey and D. M. Boore, "Beyond SaGMRotI: Conversion to SaArb, SaSN, and SaMaxRot," *Bull. Seismol. Soc. Am.*, vol. 97, no. 5, pp. 1511–1524, Oct. 2007, doi: 10.1785/0120070007.

[11] N. A. Abrahamson, "Effects of Rupture Directivity on Probabilistic Seismic Hazard Analysis," *Proc. Sixth Int. Conf. Seism. ZonationPalm Springs CA*, no. Earthquake Engineering Research Institute., pp. 151–156, 2000.

[12] P. G. Somerville, N. F. Smith, R. W. Graves, and N. A. Abrahamson, "Modification of Empirical Strong Ground Motion Attenuation Relations to Include the Amplitude and Duration Effects of Rupture Directivity," *Seismol. Res. Lett.*, vol. 68, no. 1, pp. 199–222, Jan. 1997, doi: 10.1785/gssrl.68.1.199.

[13] A. Pitarka *et al.*, "Refinements to the Graves–Pitarka Kinematic Rupture Generator, Including a Dynamically Consistent Slip-Rate Function, Applied to the 2019 Mw 7.1 Ridgecrest Earthquake," *Bull. Seismol. Soc. Am.*, Oct. 2021, doi: 10.1785/0120210138.

[14] A. A. Moya, A. Pitarka, V. Graizer, and A. Rodgers, "Simulation of Physics-Based 0-10Hz Strong Motion Using High Performance Computing Supporting Refinements to Regional Ground Motion Models for the Cent...".

[15] A. J. Rodgers, A. Pitarka, R. Pankajakshan, B. Sjögreen, and N. A. Petersson, "Regional-Scale 3D Ground-Motion Simulations of Mw 7 Earthquakes on the Hayward Fault, Northern California Resolving Frequencies 0–10 Hz and Including Site-Response Corrections," *Bull. Seismol. Soc. Am.*, vol. 110, no. 6, pp. 2862–2881, Dec. 2020, doi: 10.1785/0120200147.

[16] D. McCallen *et al.*, "An open-access simulated earthquake ground-motion database for an M7 Hayward Fault earthquake in the San Francisco Bay Region," *Earthq. Spectra*, vol. 41, no. 3, pp. 2560–2597, Aug. 2025, doi: 10.1177/87552930251340960.

[17] D. McCallen *et al.*, "Regional-scale fault-to-structure earthquake simulations with the EQSIM framework: Workflow maturation and computational performance on GPU-accelerated exascale platforms," *Earthq. Spectra*, vol. 40, no. 3, pp. 1615–1652, Aug. 2024, doi: 10.1177/87552930241246235.

[18] F. Petrone, N. Abrahamson, D. McCallen, A. Pitarka, and A. Rodgers, "Engineering evaluation of the EQSIM simulated ground-motion database: The San Francisco Bay Area region," *Earthq. Eng. Struct. Dyn.*, vol. 50, no. 15, pp. 3939–3961, Dec. 2021, doi: 10.1002/eqe.3540.

[19] C. Pinilla-Ramos, A. Pitarka, D. McCallen M. Eeri, and R. Nakata, "Performance evaluation of the USGS velocity model for the San Francisco Bay Area," *Earthq. Spectra*, vol. 41, no. 1, pp. 457–494, Feb. 2025, doi: 10.1177/87552930241270575.

[20] T. D. Ancheta, R. B. Darragh, J. P. Stewart, E. Seyhan, and W. J. Silva, "PEER NGA-West2 Database," *Pac. Earthq. Eng. Res. Cent.*, no. 03, 2013.